ELSEVIER

Journal of Molecular Structure 599 (2001) 225–237

Journal of
MOLECULAR
STRUCTURE

www.elsevier.com/locate/molstruc

The ground vibrational states of PH_2D and PHD_2[☆]

O.N. Ulenikov[a,*], H. Bürger[b], W. Jerzembeck[b], G.A. Onopenko[a],
E.S. Bekhtereva[a], O.L. Petrunina[a]

[a]*Laboratory of Molecular Spectroscopy, Physics Department, Tomsk State University, Tomsk 634050 Russian Federation*
[b]*Anorganische Chemie, FB9, Universität Gesamthochschule, D-42097 Wuppertal, Germany*

Received 10 August 2000; accepted 30 November 2000

Abstract

The high resolution (2.3–3.1×10^{-3} cm^{-1}) Far infrared Fourier transform spectrum of PH_2D and PHD_2 was recorded in the 20–160 cm^{-1} region. Assignments were made using a specially developed computer-assisted automatic 'two pair transition' method. Altogether, 1300 and 590 infrared transitions of the PHD_2 and PH_2D species, respectively, were fitted together with appropriately weighted microwave transitions to derive the rotational and centrifugal distortion parameters up to eighth order of the ground vibrational states of both molecules. The parameters obtained from these fits reproduce the microwave transitions with accuracies close to experimental uncertainties. A few of microwave transitions were shown to be blended, or misassigned. The rms deviations for the infrared data are 1.01×10^{-4} and 1.05×10^{-4} cm^{-1} for PH_2D and PHD_2, respectively, which is also close to the experimental uncertainty. © 2001 Elsevier Science B.V. All rights reserved.

Keywords: PH_3 species; Infrared; Rotational

1. Introduction

One of the main goals of high resolution vibrational–rotational spectroscopy is to define models that allow the determination of molecular spectroscopic parameters and hence accurate prediction of new transition frequencies. Generally, it may be cumbersome to find such models. However, resorting to properties of different, but related, molecules may facilitate the development of suitable models, which still preserve satisfactory predictive power. One class of molecules to which this concept can be successfully applied are so-called 'local mode molecules'. The Hamiltonian of these possesses numerous interesting and simple properties, which enable one to correctly describe vibrational–rotational spectra over wide spectral regions. For this purpose, only a rather small number of parameters is needed, see, e.g. review [1] and Ref. [2] for details.

Since most molecules are composed of, or can be prepared as, different isotopomers, it will be interesting and challenging to investigate and compare measurable properties of such different isotopic species. In recent contributions [3–8], we derived simple isotopic relations and analysed high resolution spectra of the deuterated species, D_2Se and HDSe, of the triatomic near local mode parent molecule H_2Se with C_{2v} symmetry.

[☆] This paper is dedicated to Professor Alfred Bauder in appreciation of his significant contributions to the field of microwave spectroscopy.

* Corresponding author. Fax: +7-3822-234462.
E-mail address: ulenikov@phys.tsu.ru (O.N. Ulenikov).

PII: S0022-2860(01)00826-2

Goals of our current investigations (this contribution and Refs. [9,10]) are to further develop the isotopic substitution theory and to carry out a high resolution spectroscopic study of the tetraatomic near local mode XH_3 molecules with C_{3v} symmetry. Here, the deuterated daughter species of the PH_3 molecule, PH_2D and PHD_2 with C_s symmetry, are the subjects of the study.

The phosphine molecule is an interesting target for spectroscopic studies both for purely theoretical and application-directed reasons:

(a) On one hand, phosphine plays an important role in planetology (see, e.g. Refs. [12–14], and references therein). This leads to a large interest in laboratory spectroscopic investigations of this molecule.
(b) On the other hand, the phosphine molecule is one of the lightest and simplest symmetric top molecules. Hence, spectroscopic effects and peculiarities inherent to symmetric tops should be particularly pronounced in the spectra of the phosphine molecule. At the same time, as was mentioned above, phosphine should be one of the near local mode molecules, with properties specific to such species rather well developed, [11]. Thus, PH_3 and its different isotopic species can be considered as test cases to examine the validity and correctness of different theoretical approaches, in particular, those commonly used for modeling isotopic substitution effects in near local mode XH_3 molecules.

In the past, both the pure rotational spectrum and the rotational structures of the fundamentals of PH_3, were the subjects of quite extensive studies both in the microwave and millimeterwave regions, see, for most recent work e.g. Refs. [15–17] and references cited therein, and in the infrared regions, see Refs. [18–20] and earlier work.

At the same time, surprisingly little information is available on the spectra of the deuterated species PH_2D, PHD_2 and PD_3. Only 24, 17 and 29 microwave transitions have been recorded and discussed for the PH_2D [16,21–24], PHD_2 [16,22,24], and PD_3 [16,25–27], molecules, respectively.

As to the rotationally resolved infrared spectra, there are only three contributions. In Refs. [28,29]the fundamentals ν_2, ν_{3a}, ν_{4a} and ν_{4b} of the PH_2D species investigated with an instrumental resolution of 0.005 cm^{-1} were analyzed. Of the infrared spectrum of PD_3 obtained with an instrumental resolution of about 0.06 cm^{-1} only the four fundamentals were analyzed [30]. No studies of the high resolution infrared spectrum of PHD_2 have come to our attention.

With the current contribution, we have started a thorough study of the deuterated species of the PH_3 molecule. Therefore, high resolution Fourier transform infrared spectra of PH_2D, PHD_2 and PD_3 were recorded in the wide spectral range from 20 cm^{-1} up to 5000 cm^{-1}. Experimental details are presented in Section 2.

We started our study with the lowest frequency region with the goal of determining ground state rotational energies as correct as possible. These can then be used as a basis to apply the Ground State Combination Differences method to the analysis of the rovibrational spectra.

Ground state rotational and centrifugal distortion parameters for the PH_2D species have been reported in Refs. [16,28]. However, as was already noted in [28], the value of the 1_{01}–0_{00} microwave transition of PH_2D given in Ref. [16] must be incorrect. In consequence, ground state parameters of the PH_2D species which were obtained in [16] employing also this 1_{01}–0_{00} transition frequency, cannot be considered as state-of-the-art. On the other hand, because of the higher resolution available in the present study, and the use of direct rotational transitions instead of combination differences as used in Ref. [28], we expect to obtain an improved set of ground state parameters in comparison to that reported in Ref. [28].

For PHD_2, ground state parameters have only been reported in Ref. [16]. However, analogous to the situation with PH_2D, one of the microwave transitions, namely 9_{82}–$9_{72} = 26,3757.276$ MHz, seems to be doubtful. In consequence, the ground state parameters of the PHD_2 species derived in Ref. [16] should be redetermined as well.

The present contribution is devoted to the determination of accurate ground state rotational parameters for PHD_2 and PH_2D from their high resolution Far infrared spectra. Sections 3 and 5 present the theoretical basis for the method of computer-assisted assignments of the pure rotational transitions of the PHD_2 and PH_2D species, respectively. In Sections 4 and 6, the method described in Sections 3 and 5 is applied to the newly measured pure rotational Far infrared spectra.

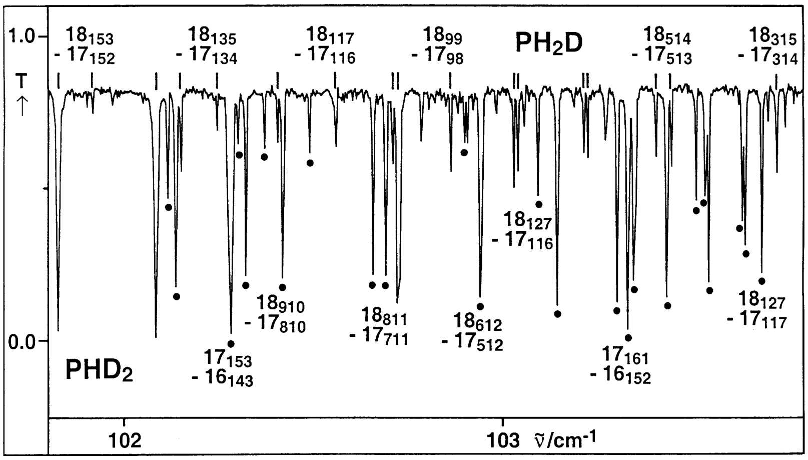

Fig. 1. Detail of the Far infrared spectrum of a mixture of PH_2D and PHD_2, resolution 0.0023 cm^{-1}, 23 μm beam splitter. Lines of PH_2D are ticked on top of the spectrum, lines of PHD_2 denoted below the spectrum by dots. Some arbitrarily selected assignments are given.

2. Experimental details

2.1. Material

Freshly prepared $[(CH_3)_3Si]_3P$ was cleaved at room temperature with 2.0 equivalents of $C_2H_5(OC_2H_4)_2OH$, and $(CH_3)_3SiPH_2$ [31] was obtained in a yield of ca. 50%. The latter was then reacted with 1.0 equivalent of $(CH_3)_3COD$, isotopic purity 99.5% -OD, and a mixture of ca. 55% PH_2D, 30% PH_3, 10% PHD_2 and 5% PD_3 was obtained in quantitative yield. Analogously $[(CH_3)_3Si]_3P$ was first cleaved with 1.35 equivalents of $(CH_3)_3COD$, then $(CH_3)_3SiPD_2$ [31] was isolated and thereafter reacted with 1.0 equivalent of $C_2H_5(OC_2H_4)_2OH$. The quantitative reaction yielded a mixture of ca. 60% PHD_2, 25% PH_2D, 10% PD_3 and 5% PH_3. Moreover, a sample of highly isotope-enriched PD_3 containing only a few % of mostly PHD_2 was available from independent work.

2.2. Spectra

Spectra were recorded at room temperature with a Bruker 120HR interferometer in the regions 20–120 and 50–320 cm^{-1}. Only PD_3 (for comparison) and the material containing ca. 60% PHD_2 and 25% PH_2D were studied; that sample provided sufficiently strong absorptions of PH_2D, too, Fig. 1, so that it deemed not necessary to record also a spectrum of the sample higher enriched in PH_2D.

A glass cell measuring 1.5 m in length of 70 mm diameter and mounted in the external parallel beam of the interferometer as reported in [32] was used. The cell was equipped with polyethylene windows, and a pressure of 6 mbar was adjusted. The interferometer was equipped with a LHe-cooled bolometer.

In the 20–120 cm^{-1} region the source was a Hg lamp, and a 23 μm Mylar beam splitter was used. The resolution (1/maximum optical path difference) was adjusted to 2.3×10^{-3} cm^{-1}, and 89 scans in total were collected.

In the 50–320 cm^{-1} region a Globar source was used, and a 6 μm Mylar beam splitter was employed. The resolution was 3.1×10^{-3} cm^{-1}, and 142 scans were coadded.

Spectra were calibrated by comparison with H_2O lines as reported in [33]. The wavenumbers of the two spectra that were analyzed are compatible with each other. Wavenumber precision is about 1×10^{-4} cm^{-1}, the accuracy of medium intensity, unblended lines is assumed to be better than 2×10^{-4} cm^{-1}.

A small portion of the 20–120 cm^{-1} spectrum is shown in Fig. 1. Lines of PH_2D are ticked on top of the spectrum, those of PHD_2 below the spectrum. Some arbitrarily selected assignments are given.

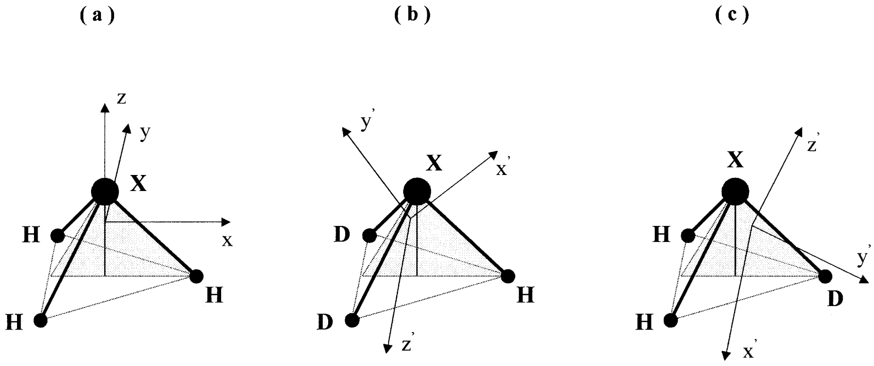

Fig. 2. Scheme of location of the frame axes in the PH_3, PHD_2 and PH_2D molecules: frame axes are directed along the main axes of inertia of molecules (see details in text).

3. The PHD_2 molecule: theoretical background of the line assignments procedure

As can be seen from Fig. 1, the recorded pure rotational spectrum is very dense, sometimes 30–40 lines/ cm^{-1}. As was mentioned in Section 1, the ground state parameters at least for the PHD_2 species may be incorrect in view of the supposedly doubtful transitions. Therefore, it is very useful to dispose of a method that provides in a correct and unambiguous procedure computer assignments of transitions belonging to the recorded dense spectrum. The background for one of such methods is discussed in the following.

First, we consider the equilibrium nuclei configuration of the parent molecule PH_3 (see Fig. 2a) and the daughter molecule PHD_2. In accordance with the general principles of vibration–rotation theory, Ref. [34], axes of a molecule fixed in a coordinate system should be directed along the main inertia axes. For the molecules under investigation here, the transformation from PH_3 to PHD_2 corresponds

(a) to a parallel translation of the coordinate origin in the '*hXH*' plane (marked on Fig. 2a)
(b) to a rotation of the x and z axes around the y axis (the z axis is the symmetry axis in PH_3; the x axis is parallel to the *H–H–H* plane and is located in the '*hXH*' plane which bisects the HPH angle).

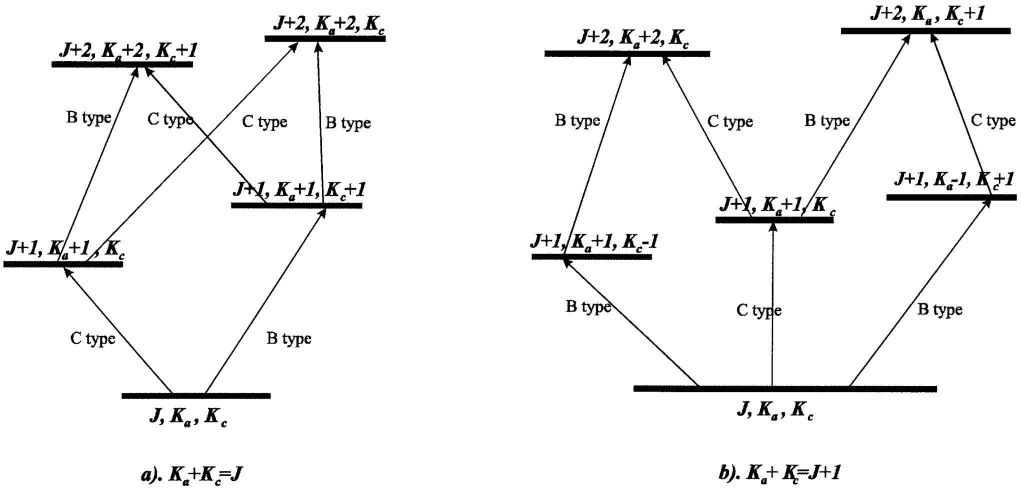

a). $K_a+K_c=J$

b). $K_a+K_c=J+1$

Fig. 3. Diagram of possible mechanisms of forming of TPT chains in the PHD_2 molecule.

Table 1
Examples of TPT twin chains in the rotational spectrum of the PHD_2 molecule

Upper			Lower			Center (cm^{-1})	Transm. (%)	Upper			Lower			Center (cm^{-1})	Transm. (%)	
J'	K'_a	K'_c	J	K_a	K_c			J'	K'_a	K'_c	J	K_a	K_c			Sum (cm^{-1})
1			2			3	4	5			6			7	8	9
9	0	9	10	1	10	43.92611	0.9	10	1	10	11	2	9	77.52098	83.7	$s1 = 121.44709$
9	0	9	10	1	9	57.89131	5.8	10	1	9	11	2	9	63.55586	3.0	$s2 = 121.44716$
16	0	16	17	1	17	73.94071	2.6	17	1	17	18	2	17	103.64492	31.7	$s1 = 177.5856$
16	0	16	17	1	16	97.97341	26.1	17	1	16	18	2	17	79.61214	6.4	$s2 = 177.58555$
24	0	24	25	1	25	107.84639	47.0	25	1	25	26	2	25	148.37269	93.5	$s1 = 256.21908$
24	0	24	25	1	24	142.85123	91.2	25	1	24	26	2	25	113.36744	77.8	$s2 = 256.21868$
8	5	4	9	4	5	44.12172	31.4	9	4	5	10	5	5	56.49008	1.1	$s1 = 100.61179$
8	5	4	9	6	4	52.25360	1.0	9	6	4	10	5	5	48.35826	48.8	$s2 = 100.61186$
25	5	20	26	6	21	118.74409	86.0	26	6	21	27	7	21	153.16436	92.8	$s1 = 271.90846$
25	5	20	26	6	20	147.67583	87.5	26	6	20	27	7	21	124.23282	91.7	$s2 = 271.90865$
11	8	3	12	9	4	70.33692	8.4	12	9	4	13	10	3	76.70547	9.8	$s1 = 147.04239$
11	8	3	12	9	3	70.40653	2.3	12	9	3	13	10	3	76.63582	3.7	$s2 = 147.04234$
19	8	11	20	9	12	98.31872	4.8	20	9	12	21	10	11	132.98608	91.3	$s1 = 231.30479$
19	8	11	20	9	11	113.16333	48.5	20	9	11	21	10	11	118.14144	57.5	$s2 = 231.30476$
15	11	4	16	12	5	93.85241	24.4	16	12	5	17	13	4	100.01264	30.1	$s1 = 193.86505$
15	11	4	16	12	4	93.86749	9.5	16	12	4	17	13	4	99.99748	15.8	$s2 = 193.86497$
21	11	10	22	12	11	114.85433	88.2	22	12	11	23	13	11	129.72036	79.9	$s1 = 244.57469$
21	11	10	22	12	10	121.87466	61.7	22	12	10	23	13	11	122.70033	93.2	$s2 = 244.57499$
22	14	8	23	15	9	131.01019	90.6	23	15	9	24	16	9	137.44900	87.1	$s1 = 268.45919$
22	14	8	23	15	8	131.19190	79.6	23	15	8	24	16	9	137.26721	93.6	$s2 = 268.45911$
23	15	8	24	16	9	137.26721	93.6	24	16	9	25	17	8	143.46440	95.5	$s1 = 280.73162$
23	15	8	24	16	8	137.33837	88.5	24	16	8	25	17	8	143.39298	92.7	$s2 = 280.73136$
18	8	10	19	9	11	94.39834	58.1	19	9	11	20	10	10	124.81267	91.1	$s1 = 219.21101$
18	8	10	19	9	10	107.18456	29.3	19	9	10	20	10	10	*112.02801	23.8	$s2 = 219.21257$

It can easily be estimated that the angle of this rotation is not far from π/4. In this case, if one calculates the values of the equilibrium rotational parameters $B^e_\alpha = h/(8\pi^2 c I^e_{\alpha\alpha})$ (here $I^e_{\alpha\alpha}$ are the equilibrium moments of inertia; $\alpha = x, y, z$), the following result is obtained. The value of the moment of inertia which corresponds to the axis out of the '*hXH*' (symmetry) plane is the smallest and close to the value of one of the two other moments of inertia. So, we assume that the condition which is usually used for asymmetric top molecules close to an oblate symmetric top, namely $A = B_z > B = B_x > C = B_y$, is fulfilled. The axes of the PHD_2 molecule obtained after the above mentioned rotation should be relabeled and placed as it is shown on Fig. 2b (i.e. the z' axis is perpendicular to the marked '*hXH*' symmetry plane).

This point is important, because it allows to conclude that in the PHD_2 molecule there are two practically equal components of the permanent dipole moment (in the parent PH_3 molecule the permanent dipole moment is directed along the z axis). In PHD_2, the dipole moment vector is located in the marked $x'y'$ plane. This means that one can expect the occurrence of two types of transitions with practically equal intensities in the Far infrared spectrum. These are *B*- and *C*-type transitions with comparable line strengths.

The above mentioned conclusion, namely the presence of two types of transitions, allows one to derive an efficient computer method for rapid assignments. The basis of this method is illustrated by the scheme Fig. 3 (from Fig. 3, one can see that the general idea of the method is very simple and similar to corresponding methods which use sums or differences of transition's wavenumbers; as the example, the traditional Ground State Combination Differences method can be mentioned). As is seen from this scheme, there are twin chains of transitions of different types all starting at the same lower rotational state $[JK_aK_c]$ and ending at the same upper rotational state $[J'K'_aK'_c]$. Clearly, the sums of the wavenumbers of the transitions belonging to a certain chain must be pairwise equal. This principle provides a firm basis for quick computer assignments of lines of PHD_2 appearing in the pure rotational spectrum. This procedure is of course independent of the values of spectroscopic parameters both of the lower and upper states, and depends only on the experimental accuracy of the line positions. It also means that, by comparing wavenumber sums of chains sharing upper and lower levels, one may estimate the experimental precision of the line positions. On the other hand, such a 'two pair transitions' (TPT) procedure allows one, beyond the assignments of spectral lines, to select suitable transitions, i.e. such which are nonblended, nonsaturated, not shifted for other reasons, etc. for the data fit. For this purpose, one should take into account only pairs of transitions whose sums of wavenumbers agree fairly well.

4. The PHD_2 molecule: assignments and discussion

The TPT procedure discussed in the Section 3 was used to construct the computer program SEARCH-II. This was used for the assignments of lines of the PHD_2 molecule in the recorded Far infrared rotational spectrum.

In the first step of the analysis, 343 TPT twin chains with values of the quantum numbers $J^{\max} = 27$ and $K_\alpha^{\max} = 17$ were extracted from the spectrum with the help of the SEARCH-II computer program. For illustration, some of such TPT twin chains with different values of involved quantum numbers J and K_a are presented in Table 1. Columns 3, 7 and 4, 8 of Table 1 give experimental values of line positions and their transmittances, respectively. Quantum numbers of the lower and upper states of the transitions are given in columns 1, 2 and 4, 5, respectively. Column 9 shows the values of the wavenumber sums of corresponding chains of the TPT procedure. The comparison of the values $s1$ and $s2$ in pairs of chains reported in Table 1 allows one to assess the experimental precision of line positions. As was estimated in Section 2, the wavenumber precision of unblended, unsaturated and not too weak lines (transmittance more than 93–94%) is about 0.00007–0.00010 cm^{-1} (see, for illustration, last column of Table 1).

Simple inspection of the values $s1$ and $s2$ in the last column of Table 1 is helpful to select those transitions which are most suitable as the starting information for solving the inverse spectroscopic problem. Provided we do not consider accidental cancellation of errors within a chain, or the same errors in both chains, transitions belonging to twin chains with values of $s1$ and $s2$ close to each other can be used without reservations. When the values $s1$ and $s2$ are not that close, an additional inspection of the data is necessary. To illustrate this, the last two lines of Table 1 give an example where such a situation is met. Here, we see that the difference between the values $s1$ and $s2$ is considerably larger than the estimated accumulation of the experimental precision of line positions. So, one should be careful in using any of the lines located at 94.39834, 124.81267, 107.18456 and 112.02801 cm^{-1}, respectively. Indeed, further analysis of these four lines reveals that the line at 112.02801 cm^{-1} which is marked in Table 1 by an asterisk is blended by another considerably stronger line. So, in the first step of the analysis, the four lines appearing in the two last lines of Table 1 were not used. Three of these lines (but not that at 112.02801 cm^{-1}) were included in the second step of the analysis (see below). In general, all the lines taking part in TPT twin chains whose differences ($s1$–$s2$) exceeded 0.0002 cm^{-1} in absolute value were omitted from the first step of the analysis.

Since states with higher values of the quantum number K_a are clustered, the TPT method was not applicable for rotational states with values of the quantum number $K_a \geq 18$. For this reason, states with $K_a \geq 18$ were not used for the determination of spectroscopic parameters in the first step of the analysis.

The above mentioned transitions belonging to the 343 TPT twin chains which satisfy the condition that $s1$ and $s2$ agree, were least-squares fitted in a first step of the analysis. As Hamiltonian model, the usual

Table 2
Ground state spectroscopic parameters for the PHD_2 molecule (in cm^{-1}) (values in parentheses are the 1σ statistical confidence intervals. Notations of parameters correspond to Eq. (1))

1	2	3
A	3.13268785(173)	3.132704198(158)
B	2.73221856(143)	2.732228719(167)
C	2.16293217(142)	2.162945246(234)
$\Delta_K \times 10^4$	0.986390(181)	0.9863227(730)
$\Delta_{JK} \times 10^4$	−0.455375(240)	−0.4549697(549)
$\Delta_J \times 10^4$	0.3724532(636)	0.3728591(186)
$\delta_K \times 10^4$	−0.3400100(494)	−0.3401298(282)
$\delta_J \times 10^4$	0.1089947(255)	0.10895370(748)
$H_K \times 10^8$	0.26829(554)	0.27827(428)
$H_{KJ} \times 10^8$	0.9885(110)	0.97303(704)
$H_{JK} \times 10^8$	−0.66071(771)	−0.64788(333)
$H_J \times 10^8$	0.18426(136)	0.189953(529)
$h_K \times 10^8$	−0.0853(167)	−0.09708(164)
$h_{JK} \times 10^8$	−0.24528(105)	−0.247351(820)
$h_J \times 10^8$	0.088861(601)	0.088304(240)
$L_K \times 10^{12}$	−1.955(160)	−2.070(166)
$L_{KKJ} \times 10^{12}$	2.707(287)	2.737(288)
$L_{JK} \times 10^{12}$	−2.360(191)	−2.211(162)
$L_{KJJ} \times 10^{12}$	0.9297(744)	0.8163(452)
$L_J \times 10^{12}$	−0.1654(101)	−0.19426(481)
$l_K \times 10^{12}$	−0.2167(657)	−0.2961(674)
$l_{KJ} \times 10^{12}$	0.0	0.0
$l_{JK} \times 10^{12}$	0.0	0.0
$l_J \times 10^{12}$	−0.07768(456)	−0.07629(228)

Watson's type operator, Ref. [35], was used:

$$\begin{aligned} H^{vv} = {} & E^v + \left[A^v - \frac{1}{2}(B^v + C^v)\right]J_z^2 + \tfrac{1}{2}(B^v + C^v)J^2 \\ & + \frac{1}{2}(B^v - C^v)J_{xy}^2 - \Delta_K^v J_z^4 - \Delta_{JK}^v J_z^2 J^2 - \Delta_J^v J^4 \\ & - \delta_K^v [J_z^2, J_{xy}^2] - 2\delta_J^v J^2 J_{xy}^2 + H_K^v J_z^6 + H_{KJ}^v J_z^4 J^2 \\ & + H_{JK}^v J_z^2 J^4 + H_J^v J^6 + [J_{xy}^2, h_K^v J_z^4 + h_{JK}^v J^2 J_z^2 \\ & + h_J^v J^4] + L_K^v J_z^8 + L_{KKJ}^v J_z^6 J^2 + L_{JK}^v J_z^4 J^4 \\ & + L_{KJJ}^v J_z^2 J^6 + L_J^v J^8 + [J_{xy}^2, l_K^v J_z^6 + l_{KJ}^v J^2 J_z^4 \\ & + l_{JK}^v J^4 J_z^2 + l_J^v J^6] \end{aligned} \tag{1}$$

with: $J_{xy}^2 = J_x^2 - J_y^2$, and $J^2 = \sum_\alpha J_\alpha^2$.

We do not report here the results of this fit, because they are only provisional and a first approximation to be further refined in the final second step of the analysis. However, it should be mentioned that the mean accuracy of reproduction of the experimental line positions was already not worse than the quoted corresponding experimental uncertainties.

In the second step of the analysis, the residual lines, i.e. those with values of the quantum number $K_a \geq 18$, and lines which did not fulfil the condition $s1 \simeq s2$ were added to the least-squares fitted data set. The rotational and centrifugal distortion parameters determined in the first step of the analysis provided excellent predictions of the positions of lines to be added. In consequence, it was easy both to select correct assignments from two pairs of transitions when $s1$ differed significantly from $s2$, and to assign unambiguously transitions belonging to the clustered states.

Finally, about 1300 pieces of data up to quantum numbers $J^{\max} = 30$ and $K_a^{\max} = 26$ were extracted from the spectrum and subjected to a least-squares fit. The parameters obtained from this fit are presented in column 2 of Table 2. Values in parentheses are 1σ confidence intervals. The rms deviation of the results is $1.02 \times 10^{-4}\ cm^{-1}$.

It is interesting to compare predictions from our results with the reported [16] microwave and millimeter wave transitions shown in column 2 of Table 3. Column 3 of Table 3 presents the values $\delta(I)$ which are the differences between the experimental line positions from column 2 and those calculated with the parameters of column 2 of Table 2. The correlation of both sets of data is satisfactory with the exception of just one transition, $9_{8\,2}$–$9_{7\,2}$. The differences $\delta(I)$ for all the other transitions are of comparable order of magnitude as the experimental uncertainties presented in parentheses in column 2 of Table 3. At the same time, the difference $\delta(I)$ for the $9_{8\,2}$–$9_{7\,2}$ transition is −37.546 MHz, which is by orders of magnitude larger than the quoted experimental uncertainty.

The final respective ground state parameters were further improved when the 16 experimental microwave transitions were added to the infrared data in the least squares fit. They were assigned weights of 100–1000 with regard to the infrared data. These weights are on purpose smaller than those calculated from the $1/\sigma^2$ relation in order to reduce the influence of possibly blended microwave transitions. The

Table 3
Microwave transitions of the PHD_2 molecule (all values are presented in MHz)

Transition 1	Exp. from Ref. [16][a] 2	$\delta(I)$ from Table 2[b] 3	$\delta(II)$ from Table 2[c] 4
$1_{1\,1}-1_{0\,1}$	12,005.030(0.030)	0.224	0.041
$1_{1\,0}-0_{0\,0}$	1,75,822.284(0.020	0.812	0.023
$1_{1\,1}-0_{0\,0}$	1,58,754.114(0.020)	0.878	0.004
$1_{1\,0}-1_{0\,1}$	29,073.210(0.050)	0.167	0.071
$2_{2\,1}-2_{1\,1}$	36,003.720(0.030)	0.555	0.023
$3_{3\,0}-3_{2\,2}$	1,11,544.084(0.050)	0.467	−0.023
$3_{2\,2}-3_{1\,2}$	19,415.190(0.050)	0.486	0.019
$4_{4\,1}-4_{3\,1}$	1,12,616.065(0.030)	1.323	−0.014
$4_{4\,0}-4_{3\,1}$	1,14,000.480(0.100)	1.225	−0.063
$5_{3\,3}-5_{2\,3}$	24,079.480(0.050)	0.714	−0.008
$6_{3\,4}-6_{2\,4}$	9049.330(0.030)	0.378	0.005
$9_{5\,5}-9_{4\,5}$	28,759.350(0.050)	0.871	0.004
$9_{8\,2}-9_{7\,2}$	2,63,757.276(0.030)	−37.546	−38.979
$11_{6\,6}-11_{5\,6}$	29,833.830(0.030)	0.742	0.012
$13_{7\,7}-13_{6\,7}$	30,531.330(0.050)	0.479	−0.018
$14_{7\,7}-14_{6\,8}$	2,54,588.040(0.030)	0.144	−0.006
$14_{7\,8}-14_{6\,8}$	11,861.050(0.050)	−0.394	−0.589

[a] Values in parentheses are the experimental uncertainties.

[b] Calculated with the parameters from column 2 of Table 2.

[c] Calculated with the parameters from column 3 of Table 2.

parameters obtained in this fit are presented in column 3 of Table 2, and differences $\delta(II)$ between the microwave observations and those calculated with the parameters of column 3 of Table 2 are given in column 4 of Table 3. The rms deviation of the infrared data is in this model close to $1.05 \times 10^{-4}\ \mathrm{cm}^{-1}$. It should be mentioned that the difference $\delta(II)$ is still very large for the $9_{8\,2}-9_{7\,2}$ transition. An attempt to incorporate the $9_{8\,2}-9_{7\,2}$ transition into the least squares fit worsens the results of the fit more than 10 times. This is convincing evidence for the conclusion that the 2,63,757.276 MHz transition was doubtfully assigned in Ref. [16].

We also believe that the 11861.050 MHz line assigned in [16] to the $14_{7\,8}-14_{6\,8}$ transition is dubious. As is evident from column 4 of Table 3, all the microwave transitions are perfectly reproduced by the parameters of column 3 of Table 2 with the exception of the above mentioned line at 2,63,757.276 MHz and the line at 11,861.050 MHz. Importantly, even a considerable increase of the number of fitted parameters did not improve the reproduction of the latter line. On this reason, we believe that the precision of the 11,861.050 MHz transition is worse than quoted in Ref. [16].

In our opinion, the present ground state rotational parameters of PHD_2 are therefore more accurate than those of Ref. [16]. Unfortunately, our Hamiltonian model differs from that of Ref. [16], and on this reason any direct comparison of the parameters is precluded. However, some more arguments underscoring the above conclusion can be put forward. First, the above mentioned unsatisfactory reproduction of the 2,63,757.276 and 11,861.050 MHz transitions which had been used in Ref. [16] as input data for the least squares fit casts doubts on the correctness of the parameters of Ref. [16]. Second, the D_J parameter in Ref. [16] was not determined from the fit but was estimated from the harmonic force field. This means that this parameter should be considered only as a first approximation to the true value. We performed some selected fits of all 17 microwave transitions with the Hamiltonian Eq. (1) and refined the same number (3 rotational, 4 quartic, and 4 sextic centrifugal distortion) of parameters as in Ref. [16]. The constrained value of the Δ_J parameter was arbitrarily and manually varied between 0.10 and

Table 4
Part of the list of the assignments in the pure rotational spectrum of PH_2D and PHD_2

Upper			Lower			Position (cm^{-1})	Transm. (%)	δ (10^{-5} cm^{-1})	Species[a]
J'	K'_a	K'_c	J'	K_a	K_c				
1			2			3	4	5	6
15	6	10	14	5	10	101.50141	10.7	7	H
18	17	1	17	17	0	101.52885	72.5	−25	H
16	3	13	15	2	13	101.58569	15.8	−13	H
14	8	6	13	7	6	101.65868	3.3	−3	H
13	10	3	12	9	3	101.82650	3.4	−22	H
18	15	3	17	15	2	101.90394	77.0	−32	H
12	12	0	11	11	0	102.08445	1.1	−31	H
22	5	17	21	6	16	102.11543	46.8	−6	D
18	8	10	17	7	10	102.13662	17.7	−14	D
18	3	16	17	3	15	102.15083	55.7	−9	H
18	13	5	17	13	4	102.24451	69.3	−6	H
18	2	16	17	2	15	102.27047	50.4	−14	H
17	15	3	16	14	3	102.28112	2.3	−4	D
21	8	13	20	9	12	102.29969	64.8	−15	D
18	10	9	17	9	9	102.32008	21.2	−4	D
21	9	13	20	8	12	102.36949	63.3	−11	D
18	12	6	17	12	5	102.40385	65.2	−12	H
18	9	10	17	8	10	102.41638	20.5	−7	D
19	11	9	18	10	8	102.48815	61.8	0	D
18	11	7	17	11	6	102.55818	63.8	−16	H
18	7	11	17	6	11	102.65689	21.6	−6	D
18	8	11	17	7	11	102.69151	21.3	−1	D
18	10	8	17	10	7	102.71044	58.1	2	H
16	5	11	15	4	11	102.72201	12.3	0	H
18	11	8	17	10	8	102.73014	20.1	−7	D
18	9	9	17	9	8	102.86453	55.6	−12	H
15	4	11	14	3	12	102.90033	65.3	37	D
18	6	12	17	5	12	102.94136	14.2	2	D
18	7	12	17	6	12	102.94430	23.8	5	D
18	8	11	17	8	10	103.02876	50.5	12	H
18	4	15	17	4	14	103.03947	55.8	−11	H
18	12	7	17	11	6	103.09225	47.7	0	D
18	6	13	17	5	13	103.14333	11.6	−11	D
18	7	12	17	7	11	103.21328	62.0	−20	H
18	7	11	17	7	10	103.22398	60.4	−10	H
18	5	14	17	4	14	103.30242	12.8	−5	D
17	16	1	16	15	2	103.33032	3.9	−7	D
18	12	6	17	11	6	103.34572	19.9	−7	D
18	6	13	17	6	12	103.40601	60.8	4	H
18	3	15	17	2	15	103.43385	14.4	−15	D
18	5	14	17	5	13	103.44682	57.5	−11	H
23	3	20	22	4	19	103.51235	46.3	−5	D
22	6	16	21	7	15	103.53581	47.7	2	D
18	6	12	17	6	11	103.53934	54.4	9	H
18	2	16	17	1	16	103.54629	19.4	−8	D
24	0	24	23	1	23	103.63682	39.7	−13	D
18	1	17	17	0	17	103.64492	31.7	−3	D
18	12	7	17	11	7	103.69027	22.5	−6	D
18	3	15	17	3	14	103.72964	55.6	−4	H

[a] In this column, H and D denote the PH_2D and PHD_2 species, respectively.

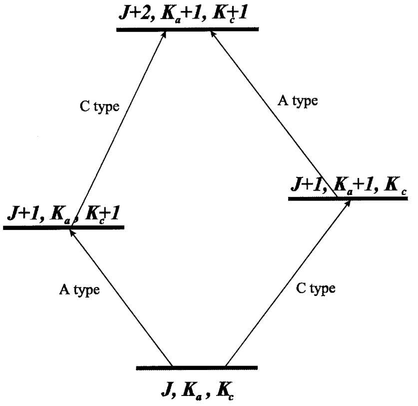

Fig. 4. Diagram of forming of TPT chains in the PH_2D molecule.

$-0.10\,\mathrm{cm}^{-1}$, i.e. in a very wide range. In all fits, experimental microwave data were equally well reproduced. This means that the reproduction of the microwave data from Ref. [16] is insensitive to the Δ_J parameter. On the other hand, the parameters of [16] fail to reproduce the infrared data even for low values of J, large discrepancies between experimental and calculated wavenumbers occurring.

In order to illustrate the reproductive quality of the refined ground state parameters, Table 4 gives some numerical information for the lines shown in Fig. 1. The values δ in column 5 of Table 4 are the differences in $10^{-5}\,\mathrm{cm}^{-1}$ between experimental line positions and those calculated with the parameters obtained in our final data fits. The agreement is excellent.

5. The PH_2D molecule: theoretical background of the line assignments procedure

Addressing the PH_2D species and considering its equilibrium nuclear configuration, arguments analogous to those presented in Section 3 lead to the following conclusions.

(a) After parallel translation of the coordinate origin in the '*hXH*' symmetry plane, the x and z axes on Fig. 2a should be rotated by an angle not too different from π/3 in order to transform the coordinate system from PH_3 to PH_2D.

(b) The equilibrium rotational constant, which corresponds to the axis directed after rotation to the substituted atom D, has the largest value; the equilibrium rotational constant which corresponds to the second axis located in the '*hXD*' symmetry plane (z' axis in Fig. 2c) is the smallest. It differs only slightly from the value of the equilibrium rotational constant, which corresponds to the axis perpendicular to the '*hXD*' plane (x' axis in Fig. 2c). This means that the PH_2D molecule is very close to a prolate symmetric top.

Table 5
Ground state spectroscopic parameters for the PH_2D molecule (in cm^{-1}) (values in parentheses are the 1σ statistical confidence intervals. Notations of parameters correspond to Eq. (1))

1	2	3
A	2.78247000(185)	2.78247196(148)
B	2.98320680(184)	2.98320620(149)
C	4.33657570(207)	4.33657995(150)
$\Delta_K \times 10^4$	−0.872605(214)	−0.873198(159)
$\Delta_{JK} \times 10^4$	0.639143(285)	0.639662(204)
$\Delta_J \times 10^4$	0.600635(150)	0.600698(108)
$\delta_K \times 10^4$	−0.777617(131)	−0.777525(862)
$\delta_J \times 10^4$	−0.0752599(478)	−0.075385(290)
$H_K \times 10^8$	−0.8913(134)	−0.90645(850)
$H_{KJ} \times 10^8$	0.3203(221)	0.3123(140)
$H_{JK} \times 10^8$	0.3697(146)	0.3896(103)
$H_J \times 10^8$	0.30482(542)	0.30497(374)
$h_K \times 10^8$	0.25008(645)	0.25038(491)
$h_{JK} \times 10^8$	−0.93034(583)	−0.92844(414)
$h_J \times 10^8$	−0.07856(228)	−0.08227(151)
$L_K \times 10^{12}$	−6.209(527)	−6.524(391)
$L_{KKJ} \times 10^{12}$	13.52(107)	14.354(798)
$L_{JK} \times 10^{12}$	−8.963(661)	−9.298(456)
$L_{KJJ} \times 10^{12}$	2.095(155)	1.9422(822)
$L_J \times 10^{12}$	−0.5076(655)	−0.4997(446)
$l_K \times 10^{12}$	−1.824(285)	−1.951(209)
$l_{KJ} \times 10^{12}$	1.638(286)	1.702(206)
$l_{JK} \times 10^{12}$	0.0	0.0
$l_J \times 10^{12}$	0.1803(300)	0.2114(203)

As will be seen from the results of the analysis to be reported below, we found that the Hamiltonian in the same form of Eq. (1) is as useful for the description of the spectrum of PH_2D as it was for PHD_2. However, the frame axes should be relabeled and denoted as shown in the figure Fig. 2c. This is compulsory because, as is well known [35], the potential of the Hamiltonian model (1) is strongly dependent on the difference between the B_x and B_y rotational constants: the larger is this difference, the more efficient is the

Table 6
Microwave transitions of the PH_2D molecule (all values are presented in MHz)

Transition from Ref. [16][a] 1	Transition from Table 5[b] 2	Exp. from Ref. [16][c] 3	$\delta(I)$ from Table 5[d] 4	$\delta(II)$ from Table 5[e] 5
$1_{1\,1}$–$1_{0\,1}$	$1_{1\,1}$–$1_{1\,0}$	40,561.870(0.050)	−0.070	−0.117
$1_{1\,0}$–$1_{1\,1}$	$1_{0\,1}$–$1_{1\,1}$	6024.645(0.005)	0.026	0.004
$1_{0\,1}$–$0_{0\,0}$	$1_{1\,0}$–$0_{0\,0}$	1,72,524.933(0.015)	−322.816	−322.846
$2_{1\,2}$–$2_{0\,2}$	$2_{2\,1}$–$2_{2\,0}$	35,142.100(0.030)	0.215	0.021
$2_{1\,1}$–$2_{1\,2}$	$2_{1\,1}$–$2_{2\,1}$	18,070.910(0.035)	−0.241	−0.024
$3_{1\,2}$–$3_{1\,3}$	$3_{2\,1}$–$3_{3\,1}$	36,093.670(0.030)	−0.398	0.020
$3_{1\,3}$–$3_{0\,3}$	$3_{3\,1}$–$3_{3\,0}$	28,158.500(0.030)	0.236	−0.001
$3_{2\,2}$–$3_{1\,2}$	$3_{2\,2}$–$3_{2\,1}$	1,12,977.568(0.050)	0.478	0.009
$4_{1\,4}$–$4_{0\,4}$	$4_{4\,1}$–$4_{4\,0}$	20,815.334(0.005)	0.250	0.000
$5_{1\,5}$–$5_{0\,5}$	$5_{5\,1}$–$5_{5\,0}$	14,246.690(0.010)	0.223	−0.002
$5_{2\,3}$–$5_{2\,4}$	$5_{3\,2}$–$5_{4\,2}$	19,611.360(0.100)	−0.117	0.074
$6_{1\,6}$–$6_{0\,6}$	$6_{6\,1}$–$6_{6\,0}$	9121.376(0.005)	0.179	0.001
$6_{2\,4}$–$6_{2\,5}$	$6_{4\,2}$–$6_{5\,2}$	36,331.040(0.040)	−0.307	−0.039
$7_{1\,7}$–$7_{0\,7}$	$7_{7\,1}$–$7_{7\,0}$	5536.382(0.003)	0.129	0.002
$9_{2\,8}$–$9_{1\,8}$	$9_{8\,2}$–$9_{8\,1}$	30,957.770(0.030)	0.279	0.015
$10_{4\,7}$–$10_{3\,7}$	$10_{7\,4}$–$10_{7\,3}$	2,56,864.972(0.015)	−0.112	0.001
$10_{3\,8}$–$10_{2\,8}$	$10_{8\,3}$–$10_{8\,2}$	1,12,617.504(0.030)	0.041	−0.019
$10_{2\,9}$–$10_{1\,9}$	$10_{9\,2}$–$10_{9\,1}$	20,754.570(0.050)	0.468	0.282
$11_{2\,10}$–$11_{1\,10}$	$11_{10\,2}$–$11_{10\,1}$	13,259.560(0.030)	0.111	−0.018
$14_{3\,12}$–$14_{2\,12}$	$14_{12\,3}$–$14_{12\,2}$	34,520.190(0.030)	0.009	0.008
$15_{3\,13}$–$15_{2\,13}$	$15_{13\,3}$–$15_{13\,2}$	22,821.900(0.050)	0.032	−0.059
$16_{3\,14}$–$16_{2\,14}$	$16_{14\,3}$–$16_{14\,2}$	14,504.990(0.040)	0.153	0.003
$17_{3\,15}$–$17_{2\,15}$	$17_{15\,3}$–$17_{15\,2}$	8916.190(0.060)	0.234	0.068
$19_{4\,16}$–$19_{3\,16}$	$19_{16\,4}$–$19_{6\,3}$	34,207.180(0.050)	0.879	0.002

[a] Notations of transitions correspond to Ref. [16].
[b] Notations of transitions correspond to Hamiltonian model of Table 5.
[c] Values in parentheses are the experimental uncertainties.
[d] Calculated with the parameters from column 2 of Table 5.
[e] Calculated with the parameters from column 3 of Table 5.

model. Therefore, the model with an order of the rotational parameters $B_z > B_x > B_y$ is not applicable to PH_2D, because the $(B_x - B_y)$ value is very small. On the other hand, one can expect that the axis notation shown on Fig. 2c (in this case the condition $B_y > B_x > B_z$ is fulfilled) will lead to a model that is even more efficient than that employed in Section 4 for PHD_2. This follows from the fact that the value of the difference $(B_x - B_y)$ is $0.57\ \mathrm{cm}^{-1}$ for the PHD_2 molecule (see Table 2), while it is $1.35\ \mathrm{cm}^{-1}$ in absolute value for PH_2D (see Table 5) when the axes x', y' and z' are chosen as on Fig. 2c. In this case, the following remark should be made: the situation with the PH_2D molecule now looks like the III^l representation in asymmetric top molecules (see, [36]). However, we assume that, as usually, the molecular fixed coordinate axes are right-handed ones and keep the notations of the Hamiltonian parameters in the form of Eq. (1).

As for the PHD_2 molecule, rotation of the frame axes from the PH_3 configuration shown in Fig. 2a to the configuration illustrated in Fig. 2c enables one to predict that in PH_2D both *A*- and *C*-type transitions should occur with comparable intensities. This, in turn, offers the basis to derive a procedure for straightforward computer-assisted assignments of transitions belonging to the pure rotational spectrum of PH_2D. The scheme for the corresponding TPT method for the PH_2D molecule is shown in Fig. 4. As described for PHD_2, the computer program SEARCH-II was modified in such a way that it enabled to successfully assign many ground state transitions of PH_2D appearing in the recorded spectrum.

6. The PH_2D molecule: assignments and discussion

We will not repeat here step-by-step the procedure of the assignment of transitions, because it is very similar to that described in Section 4, and we will draw our attention mostly to the results of the analysis.

The use of the TPT method enabled us to assign in the present case 592 transitions up to values of the quantum numbers $J^{\max} = 26$ and $K_a^{\max} = 26$. The precision of most of these transitions was estimated to be 0.00009–0.00011 cm^{-1} by comparison of the values $s1$ and $s2$ as mentioned in Section 4. Least squares fits of all these experimental transitions led to the set of parameters which is presented in column 2 of Table 5. The rms deviation of the fit was $0.99 \times 10^{-4}\ cm^{-1.}$

As for the PHD_2 molecule, it is interesting to estimate the quality of the obtained results by comparison of calculated and experimental values of the microwave transitions from Ref. [16]. A list of these experimental values is given in column 3 of Table 6, and column 3 presents the values $\delta(I)$ which are the differences between the values of column 3 and those calculated with the parameters of column 2 of Table 5. All $\delta(I)$ values are comparable with the experimental uncertainties, which are given in parentheses in column 2, with the exception of the $1_{1\,0}$–$0_{0\,0} = 1,72,524.933$ MHz transition. As was mentioned in [28], this latter line from Ref. [16] is doubtful, and the results of our analysis confirm that observation.

In the final step of the analysis, the microwave data on PHD_2 from Ref. [16]were fitted together with the Far infrared data. The results of this merged fit are presented in column 3 of Table 5.

The microwave data were again assigned weights of 100–1000 for the same reasons as mentioned for PHD_2. The rms deviation of the fitted infrared data was then $1.01 \times 10^{-4}\ cm^{-1}$. Column 5 of Table 6 reports the differences between the experimental microwave transitions and their values calculated with the parameters of Table 5, column 3. The $\delta(II)$ values and the corresponding experimental uncertainties are consistent with the exception of two transitions, $1_{1\,1}$–$1_{1\,0} = 40,561.870$ MHz and $10_{9\,2}$–$10_{9\,1} = 20,754.570$ MHz However, if one looks at Table I of Ref. [16], one realizes that those two transitions have practically the same deviations as in the Table 6 of the present study. This confirms that the mentioned unusually large deviations are not due to the fit but attributable to the data.

7. Conclusions

The high resolution (2.3–$3.1 \times 10^{-3}\ cm^{-1}$) Far infrared Fourier transform spectrum of a mixture mostly consisting of PH_2D and PHD_2 was recorded in the 20–160 cm^{-1} region for the first time and assigned with the help of a specially developed computer-assisted 'two pair transition' (TPT) method. The measured 1300 and 590 infrared transitions of PHD_2 and PH_2D, respectively, were fitted together with microwave transitions reported in the literature to yield substantially improved rotational and centrifugal distortion parameters of the ground vibrational states of both molecules. The parameters obtained from these fits reproduce the microwave data with accuracies comparable to the quoted experimental uncertainties. Some dubious microwave transitions have been detected. The rms deviations for the infrared data are 1.01×10^{-4} and $1.05 \times 10^{-4}\ cm^{-1}$ for PH_2D and PHD_2, respectively, which is close to the experimental uncertainties. The improved ground state constants will be useful for ongoing work on the rotational structure of vibrationally excited states of PHD_2 and PH_2D, in particular in the domain of transitions with large rotational quantum numbers.

Acknowledgements

We thank the Deutsche Forschungsgemeinschaft and ministry for High Education of Russian Federation for financial support.

References

[1] M.S. Child, L. Halonen, Adv. Chem. Phys. 57 (1984) 1.
[2] T. Lukka, L. Halonen, J. Chem. Phys. 101 (1994) 8380.
[3] O.N. Ulenikov, G.A. Onopenko, N.E. Tyabaeva, H. Bürger, W. Jerzembeck, J. Mol. Spectrosc. 197 (1999) 100.
[4] J.-M. Flaud, Ph. Arcas, O.N. Ulenikov, G.A. Onopenko, N.E. Tyabaeva, H. Bürger, W. Jerzembeck, J. Mol. Spectrosc. 197 (1999) 212.
[5] W. Jerzembeck, H. Bürger, J.-M. Flaud, Ph. Arcas, J. Mol. Spectrosc. 197 (1999) 215.
[6] O.N. Ulenikov, G.A. Onopenko, N.E. Tyabaeva, H. Bürger, W. Jerzembeck, J. Mol. Spectrosc. 198 (1999) 27.

[7] O.N. Ulenikov, H. Bürger, W. Jerzembeck, G.A. Onopenko, E.A. Zhabina, O.L. Petrunina, J. Mol. Spectrosc. 202 (2000) 229.

[8] O.N. Ulenikov, H. Bürger, W. Jerzembeck, G.A. Onopenko, E.A. Zhabina, V.A. Kozinskaia, J. Mol. Spectrosc. 203 (2000) 132.

[9] O.N. Ulenikov, H. Bürger, W. Jerzembeck, G.A. Onopenko, V.V. Melnikov, O.L. Petrunina, High Resolution Study of the Lowest Energy Fundamental Bands of PHD_2, in preparation.

[10] O.N. Ulenikov, H. Bürger, W. Jerzembeck, G.A. Onopenko, E.A. Sinitsin, E.S. Bekhtereva, J. Mol. Spectrosc 209 (2001).

[11] O.N. Ulenikov, R.N. Tolchenov, Qing-shi Zhu, Spectrochim. Acta A53 (1997) 845.

[12] A.T. Tokunaga, R.F. Knacke, S.T. Ridgway, L. Wallace, Astrophys. J. 232 (1979) 603.

[13] R.F. Knacke, S.J. Kim, S.T. Ridgway, A.T. Tokunaga, Astrophys. J. 262 (1982) 388.

[14] L.-M. Lara, B. Bezard, C.A. Griffith, J.H. Lacy, T. Owen, ICARUS 131 (1988) 317.

[15] M. Carlotti, G. Di Lonardo, A. Trombetti, J. Chem. Phys. 78 (1983) 1670.

[16] G.A. McRae, M.C.L. Gerry, E.A. Cohen, J. Mol. Spectrosc. 116 (1986) 58.

[17] Y.-T. Chen, T. Oka, J. Mol. Spectrosc. 133 (1989) 148.

[18] A.V. Burenin, L. Fusina, M. Carlotti, J. Mol. Spectrosc. 160 (1993) 97.

[19] A. Ainetschian, U. Häring, G. Spiegl, W.A. Kreiner, J. Mol. Spectrosc. 181 (1996) 99.

[20] M. Jackson, G.R. Sudhakaran, E. Gansen, J. Mol. Spectrosc. 181 (1997) 446.

[21] C.C. Loomis, M.W.P. Strandberg, Phys. Rev. 81 (1951) 798.

[22] M.H. Sirvetz, R.E. Weston, J. Phys. Chem. 21 (1953) 898.

[23] S.G. Kukolich, L. Schaum, A. Murray, J. Mol. Spectrosc. 94 (1982) 393.

[24] D.C. McKean, I. Torto, A.R. Morrisson, J. Phys. Chem. 86 (1982) 307.

[25] P. Helminger, W. Gordy, Phys. Rev. 188 (1969) 100.

[26] F.Y. Chu, T. Oka, J. Chem. Phys. 60 (1974) 4612.

[27] D.A. Helms, W. Gordy, J. Mol. Spectrosc. 66 (1977) 206.

[28] R.J. Kshirsagar, V.A. Job, J. Mol. Spectrosc. 161 (1993) 170.

[29] R.J. Kshirsagar, V.A. Job, J. Mol. Spectrosc. 185 (1997) 272.

[30] K. Kijima, T. Tanaka, J. Mol. Spectrosc. 89 (1981) 62.

[31] H. Bürger, U. Goetze, J. Organomet. Chem. 12 (1968) 451.

[32] M. Birk, M. Winnewisser, E.A. Cohen, J. Mol. Spectrosc. 136 (1989) 402.

[33] G. Guelachvili, K. Narahari Rao, Handbook of Infrared Standards, Academic Press, San Diego, 1986.

[34] D. Papoušek, M.R. Aliev, Molecular Vibration–Rotation Spectra, Elsevier, Amsterdam, 1982.

[35] J.K.G. Watson, J. Chem. Phys. 46 (1967) 1935.

[36] G.W. King, R.M. Hainer, P.C. Cross, J. Chem. Phys. 11 (1943) 27.